Received: 19 May 2022 | Revised: 13 August 2022 | Accepted: 18 August 2022

DOI: 10.1002/jbm.a.37444

RESEARCH ARTICLE

Society For Biomaterials | WILEY

Proteomic evaluation of human osteoblast responses to titanium implants over time

Francisco Romero-Gavilán[1] | Andreia Cerqueira[1] | Iñaki García-Arnáez[2] | Mikel Azkargorta[3] | Félix Elortza[3] | Mariló Gurruchaga[2] | Isabel Goñi[2] | Julio Suay[1]

[1]Department of Industrial Systems Engineering and Design, Universitat Jaume I, Castellón de la Plana, Spain

[2]Department of Polymers and Advanced Materials: Physics, Chemistry and Technology, Universidad del País Vasco, San Sebastián, Spain

[3]Proteomics Platform, CIC bioGUNE, Basque Research and Technology Alliance (BRTA), CIBERehd, ProteoRed-ISCIII, Bizkaia Science and Technology Park, Derio, Spain

Correspondence
Francisco Romero-Gavilán, Departamento de Ingeniería de Sistemas Industriales y Diseño, Campus del Ríu Sec, Avda. Vicent Sos Baynat s/n, 12071 Castelló de la Plana, Spain.
Email: gavilan@uji.es

Funding information
Euskal Herriko Unibertsitatea, Grant/Award Number: GIU18/189; Generalitat Valenciana, Grant/Award Numbers: APOSTD/2020/036, PROMETEO/2020/069; Ministerio de Ciencia e Innovación, Grant/Award Number: PID2020-113092RB-C21; Universitat Jaume I, Grant/Award Number: UJI-B2021-25

Abstract

Titanium is widely used in bone prostheses due to its excellent biocompatibility and osseointegration capacity. To understand the effect of sandblasted acid-etched (SAE) Ti implants on the biological responses of human osteoblast (HOb), their proteomic profiles were analyzed using nLC-MS/MS. The cells were cultured with the implant materials, and 2544 distinct proteins were detected in samples taken after 1, 3, and 7 days. Comparative analyses of proteomic data were performed using Perseus software. The expression of proteins related to EIF2, mTOR, insulin-secretion and IGF pathways showed marked differences in cells grown with SAE-Ti in comparison with cells cultured without Ti. Moreover, the proteomic profiles obtained with SAE-Ti were compared over time. The affected proteins were related to adhesion, immunity, oxidative stress, coagulation, angiogenesis, osteogenesis, and extracellular matrix formation functions. The proliferation, mineralization and osteogenic gene expression in HObs cultured with SAE-Ti were characterized in vitro. The results showed that the osteoblasts exposed to this material increase their mineralization rate and expression of COLI, RUNX2, SP7, CTNNB1, CAD13, IGF2, MAPK2, and mTOR. Overall, the observed proteomic profiles can explain the SAE-Ti osteogenic properties, widening our knowledge of key signaling pathways taking part in the early stages of the osseointegration process in this type of implantations.

KEYWORDS
cell-material interaction, dental implants, molecular biocompatibility, mTOR signaling, osseointegration

1 | INTRODUCTION

The development of titanium (Ti) screw implant by Brånemark in 1965 was a stepping stone in modern oral implantology.[1] Since then, Ti has become the gold-standard material in implant dentistry. The commercially pure Ti (CP Ti) and its alloys have also been widely used to construct other orthopedic devices such as mini-screws, artificial joints, bone plates, wire, bone nails, and spinal fixators.[2]

Ti is one of the best materials for implants due to its favorable characteristics: good mechanical properties, chemical stability, and excellent biocompatibility.[3] The interaction of Ti with tissues is governed by the properties of the oxide layer covering the substrate, formed by the passivation process. The corrosion resistance of this layer explains the non-toxic nature of this material.[4] The good compatibility between Ti and hard tissues is now widely accepted after many years of research and clinical use. Many in-vitro studies have

demonstrated that Ti can promote the adhesion and proliferation of osteoblastic cells, as well as their mineralization.[5] Furthermore, the ability of Ti implants to achieve osseointegration has been reported in vivo and in clinical evaluations.[6,7] Overall, these studies demonstrate the positive effect of Ti on bone tissue regeneration. However, the mechanism by which Ti achieves its superior biocompatibility and osseointegration in comparison with other metallic materials is not fully understood.[2]

Ti is considered bioinert; many research efforts have focused on developing and studying novel surface modifications designed to bioactivate the Ti implants and thus improve their biological responses favoring the osseointegration.[6,8,9] Among these modifications, increasing surface roughness by combining grit-blasting and acid-etching treatments has enhanced clinical performance and is currently widely used in dental implantology.[6,10] Any material implantation into a human body causes an immediate reaction in the living tissue, triggering various biological responses. This initial interaction between the implanted materials and tissues conditions the final outcome of the healing process.[11] Therefore, a thorough exploration of the effect of implanted materials on living cells is necessary. Many physiological phenomena in osteogenic cells, observed at the molecular level, might affect the efficacy of the regeneration process around Ti implants.[12] Improving our knowledge of molecular interactions between the cell and Ti surfaces should provide the basis for predicting the biological behavior of new materials. However, so far, the attempts to evaluate the effect of Ti on the biological response to the implants have been limited by traditional methods and have focused on just a few genes and proteins related to osteoblast proliferation, differentiation or matrix formation.[13]

Proteomics allows a large-scale identification and quantification of proteins, providing an improved global view of molecular mechanisms in the regeneration processes triggered by biomaterials.[14,15] This can help in understanding the dynamic responses of cells to implanted materials. For instance, Othman et al.[16] have examined and compared the proteomic profiles of human mesenchymal stromal cells (hMSCs) cultured on non-osteoinductive hydroxyapatite (HA) and osteoinductive β-tricalcium phosphate (TCP) ceramic particles. The hMSCs exposed to TCP upregulated mainly the proteins related to wound healing, cell proliferation, and extracellular matrix formation. The HA induced the expression of proteins associated with protein production, translation, localisation, and secretion processes. Using matrix-assisted laser desorption/ionization time-of-flight mass spectrometry (MALDI-TOF-MS), Kim et al.[17] have analyzed the differences between protein expression profiles of MG63 osteoblasts cultured on three distinct surface materials. The authors have used smooth Ti, sand-blasted and acid-etched Ti (SLA) and Ti coated with HA. They have demonstrated that the variations in surface properties of these materials affect the expression of proteins involved in osseointegration. Zhao et al.[18] have used proteomics to compare the cellular response of MG63 osteoblasts cultured with CP Ti and polyetheretherketone (PEEK). The two materials cause similar patterns of changes in the regulation of biosynthesis, metabolism and cell adhesion, consistent with their bioinert behavior. The PEEK causes greater inhibition in mRNA processing than CP Ti, which explains the lower proliferation rate of cells incubated with this material. The proteome profiles of human primary osteoblasts cultured with Ti and high-purity magnesium were analyzed and compared by Omidi et al.[19] The results of this study confirm that both materials had individual effects on osteoblasts, which were mirrored by changes in the protein patterns. Comparing protein expression profiles of MG-63 osteoblasts grown in contact with nanostructured Ti and CP Ti shows that the latter can have a beneficial effect; it can prevent oxidative damage to the cells by upregulating superoxide dismutase 2.[20] However, the analysis over time of changes in protein expression in cells exposed to biomaterials has not been fully addressed.

This study presents a thorough nLC-MS/MS evaluation of proteomic profile changes in HOb cells cultured on the SAE CP Ti for 1, 3, and 7 days. The protein expression of these cells was measured after each of those periods and compared to the profiles of the cells cultured in polystyrene wells without these materials, normally used as controls in in vitro tests. In addition, a comparison between the results obtained at different times was carried out to analyze the evolution of the proteomic profiles with the cultivation time. The correlation of the HOb protein expression with the proliferative capability and the osteogenic potential in vitro was also examined. The results presented here should improve the understanding of the biological response to Ti surfaces at the proteomic level and the effect of these materials on the osseointegration process.

2 | MATERIALS AND METHODS

2.1 | Sample preparation

The surfaces of grade-4 Ti discs (1-mm thick and 10 mm in diameter; GMI Ilerimplant SL., Lleida, Spain) were modified by sand-blasting and acid-etching (SAE; GMI Ilerimplant SL.), following the procedures described previously.[21] Then, the samples were sterilized by γ-irradiation.

2.2 | Proteomic evaluation

2.2.1 | Cell culture

Human osteoblasts (HOb) derived from healthy bone (Cell Applications Inc., San Diego, CA) were expanded in a proliferation medium. The medium was prepared by supplementing low-glucose Dulbecco's Modified Eagle's Medium with 0.584 g L^{-1} L-glutamine (DMEM; Merck, Darmstadt, Germany), foetal bovine serum (10%; FBS; Merck), and penicillin/streptomycin (100 U ml^{-1}; Gibco, Thermo Fisher Scientific, Waltham, MA). FBS was used instead of human serum aiming to distinguish between the human proteins produced by the cells and the bovine proteins adsorbed onto the surface. The osteoblasts were seeded at the density of 2.5×10^4 per cm^2 on the SAE-Ti samples in a 48-well plate with osteogenic medium (DMEM, 1% penicillin/streptomycin, 10% FBS, 1% ascorbic acid [5 μg ml^{-1}; Merck] and β-glycerol

phosphate [100 mM; Merck]). The cells were cultured for 1, 3, and 7 days in a humidified atmosphere (37°C, 5% CO_2). Cells cultured in polystyrene wells without Ti discs were used as control (C). The cell culture medium was changed every 3 days.

2.2.2 | Protein digestion

The HOb cells were seeded and cultured as described above (Section 2.3.1). Then, they were washed four times with phosphate-buffered saline (PBS; Merck). Next, the cells were lysed using lysis buffer (2 M thiourea, 7 M urea, 4% CHAPS, 200 mM dithiothreitol; Merck) by keeping the samples in the lysis buffer under agitation (280 rpm) for 30 min. The lysate was collected and centrifuged at 13,000 rpm for 30 min at 4°C. The supernatant was separated and stored at −80°C until further analysis. Four independent samples ($n = 4$) were used for each condition; each of these samples was made by pooling the lysate from three wells. In this assay, the cells were cultured with FBS and osteogenic medium (standard for HOb in vitro testing).

Protein was digested following the filter-aided FASP protocol described by Wisniewski et al.[22] with minor modifications. Trypsin was added to a trypsin: protein ratio of 1:20, and the mixture was incubated overnight at 37°C, dried out in a RVC2 25 speedvac concentrator (Christ, Osterode/Harz, Germany), and resuspended in 0.1% FA. Peptides were desalted using C18 stage tips (Merk Millipore, Burlington, MA) and resuspended in 0.1% FA.

2.2.3 | Protein identification and bioinformatic data analysis

Proteomic analysis was performed by loading 200 ng of the purified and resuspended in 0.1% FA sample (obtained from Section 2.2.2) onto an Evosep One chromatograph (Evosep Biosystems, Odense C, Denmark) coupled to a hybrid trapped ion mobility spectrometer—quadrupole time-of-flight mass spectrometer (timsTOF Pro with PASEF; Bruker, Billerica, MA). Evosep 30 SPD protocol was applied (44 min gradient) and a 15 cm column (Evosep) was used. The timsTOF Pro was operated in DDA mode using the Standard 1.1s cycle time acquisition mode. Each sample was evaluated in quadruplicate. The mass spectrum raw dataset was examined using the MaxQuant programme (http://maxquant.org/), and the Perseus software platform (https://www.maxquant.org/perseus/) was employed for label free comparative analysis. Only proteins identified with at least two different peptides (one of the unique to that protein group) at FDR1% (PSM-level) were considered in the analysis. LFQ intensities were used for the quantitative analysis of proteins. To examine the effects of Ti on the osteoblast protein expression, proteomic profiles of HOb cells cultured with SAE-Ti samples were compared with those obtained for controls (C). To evaluate the alterations in protein expression over time, proteomic profiles of SAE-Ti samples at 1 day of culture were compared with the results obtained for 3 and 7 days. The protein expression was considered different at $p \leq .05$ (Student's t-test), and the ratio of abundances for the compared conditions higher than 1.5 in either direction (UP: increased and DOWN: reduced).

The functional classification of differentially upregulated and downregulated proteins was carried out using the PANTHER classification system (http://www.pantherdb.org/). DAVID v6.8 (Database for Annotation, Visualisation and Integrated Discovery, https://david.ncifcrf.gov/) was used to identify enriched functional clusters. STRING v.11.5 (Search Tool for the Retrieval of Interacting Genes/Proteins; https://string-db.org/) was employed to generate protein–protein interaction networks, connecting the linked proteins to their associated gene ontology (GO) terms. Only the interactions with high confidence scores were considered. Moreover, relative pathway analysis of differentially altered proteins was performed using Ingenuity Pathway Analysis (IPA; Ingenuity System, Redwood City, CA) software. The Canonical Pathways tool was used to obtain the probability that a pathway was significantly more active in cells cultured on SAE-Ti discs than in control wells; the diagrams were built employing the Molecule Activity Predictor tool. This procedure was used with a specific focus on osteoblast-related pathways and molecules.

2.3 | In-vitro experimentation

2.3.1 | Cell proliferation and mineralization

HOb cells were cultured as was described in *Cell culture* section and seeded in 48-well plates at 1×10^4 cm^{-2}. Cell proliferation was measured using the CellTiter 96® Proliferation kit (MTS; Promega, Madison, WI). The proliferation was evaluated following the manufacturer's instructions, measuring the absorbance at 490 nm in a microplate reader (Multiskan FC, Thermo Fisher Scientific, Waltham, MA) after 1, 3, and 7 days of culture. The HOb mineralization capability was assessed using Alizarin Red S (ARS) to quantify calcium deposits after 7 and 14 days of culture. The ARS was extracted with cetylpyridinium chloride in 10 mM Na_2HPO_4 (pH 7.0) and measured at 540 nm. Three independent samples were analyzed for each condition in each assay.

2.3.2 | Quantitative real-time PCR

The expression of osteogenic genes was measured by quantitative real-time PCR (qRT-PCR). The HOb osteoblasts were cultured as explained before and seeded at 2.5×10^4 cells cm^{-2} for 1, 3, and 7 days. Total RNA extraction was performed using the TRIzol method, following the protocol described in Cerqueira et al.[23] A NanoVue® Plus Spectrophotometer (GE Healthcare Life Sciences, Little Chalfont, UK) was employed to measure the RNA concentration and quality. Then, RNA (500 ng) was turned into cDNA using PrimeScript RT Reagent Kit (Perfect Real Time; TAKARA Bio Inc., Shiga, Japan). cDNA samples were stored at −20°C until their analysis, and qRT-PCR measurements were carried out in a StepOne Plus™ Real-Time PCR System (Applied Biosystems®, Thermo Fisher Scientific) as described in Cerqueira et al.[23] Briefly, the reaction conditions were 95°C for 30 s, followed by

TABLE 1 Targets studied in HOb cells

Name	Accession	Sequence	Product length
GAPDH (*GAPDH*)	NM_001357943.2	F: GAGTCAACGGATTTGGTCGT R: TTGATTTTGGAGGGATCTCG	184
Collagen I (*COLI*)	JQ236861.1	F: GTGCTAAAGGTGCCAATGGT R: ACCAGGTTCACCGCTGTTAC	128
Runt-related transcription factor 2 (*RUNX2*)	NM_001015051.4	F: TTTGCACTGGGTCATGTGTT R: TGGCTGCATTGAAAAGACTG	156
Osterix (*SP7*)	NM_001300837.2	F: GCCAGAAGCTGTGAAACCTC R: AGGGAGATGGGGTACATTCC	65
β-Catenin (*CTNNB1*)	NM_001330729	F: ACCTTTCCCATCATCGTGAG R: AATCCACTGGTGAACCAAGC	90
Cadherin-13 (*CAD13*)	L34058.1	F: ATACACACGCCCTGGTAAGC R: ATGGGCAGGTTGTAGTTTGC	60
Insulin growth factor 2 (*IGF2*)	NM_001007139	F: GGGAGTTCTGGGGTAGGAAG R: TGCAAGTCTGCTGTCAATCC	74
Alkaline phosphatase (*ALP*)	NM_001127501.4	F: CCACGTCTTCACATTTGGTG R: AGACTGCGCCTGGTAGTTGT	196
Mitogen-activated protein kinase (*MAPK2*)	NM_030662.4	F: GTGCTGAAAGAGGCCAAGAG R: GTGCTTCTCTCGGAGGTACG	93
Mammalian target of rapamycin (*mTOR*)	NM_001386500	F: CCAACAGTTCACCCTCAGGT R: GGGCACTCTTCCACATGTTT	58

40 cycles of 95°C for 5 s, 60°C for 34 s, 95°C for 15 s and 60°C for 60 s. The targets studied are shown in Table 1. Results were normalized to GAPDH housekeeping gene and C samples using the $2^{-\Delta\Delta Ct}$ method. Six technical replicates were analyzed for each condition.

2.3.3 | Statistical analysis

GraphPad Prism® (version 5.04; GraphPad Software Inc., La Jolla, CA) one-way variance analysis (ANOVA) with Tukey post hoc test was employed to perform statistical analysis. Differences were considered statistically significant at $p \leq .05$ (*), $p \leq .01$ (**), and $p \leq .001$ (***). Differences between SAE-Ti and C were marked with (*), while differences between SAE-Ti at 1 day and after 3 and 7 days were marked with (♦). Proliferation and mineralization were evaluated in triplicate. Regarding qRT-PCR assays, four samples were tested for each condition and six technical replicates were analyzed in each measurement. In-vitro results were expressed as mean ± standard error (SE).

3 | RESULTS

3.1 | HOb proteomic profile analysis

Identification and quantification of proteins in the lysed HOb cells cultured on SAE-Ti and C were carried out using the MaxQuant package. Two thousand five hundred forty-four different human proteins were identified in the samples. The Perseus analysis of proteomic results from osteoblasts cultured on SAE-Ti in comparison with C samples, for each time point, detected the UP/DOWN differentially expressed proteins in the cells grown in contact with the SAE-Ti material (Table S1). Table 2 shows the number of UP and DOWN proteins expressed over time, revealed in this comparative analysis. After 1 day of culture, 616 proteins were differentially expressed. After 3 and 7 days, 221 and 413 such proteins were identified, respectively.

TABLE 2 UP, DOWN and the total number of proteins detected as differentials in the comparative analysis of the proteomic profiles of HOb cells cultured on SAE-Ti compared with C

Time	Day 1	Day 3	Day 7
UP	48	24	94
DOWN	568	197	319
Total	616	221	413

To examine the changes in protein expression during the 7-day incubation, we compared protein profiles of osteoblastic cells in contact with SAE-Ti for 1 day with those cultured 3 and 7 days (Table S2). The analysis detected 304 differentially expressed proteins (70 UP and 234 DOWN) after 3-day culture (in comparison with cells incubated for 1 day). A similar comparison for the 7-day culture revealed 755 differentially expressed proteins (115 UP and 640 DOWN).

3.2 | Functional classification of differential proteins: SAE-Ti versus C

3.2.1 | PANTHER classification

The PANTHER classification system was used to analyze the differentially expressed proteins and detect the associated functions. The

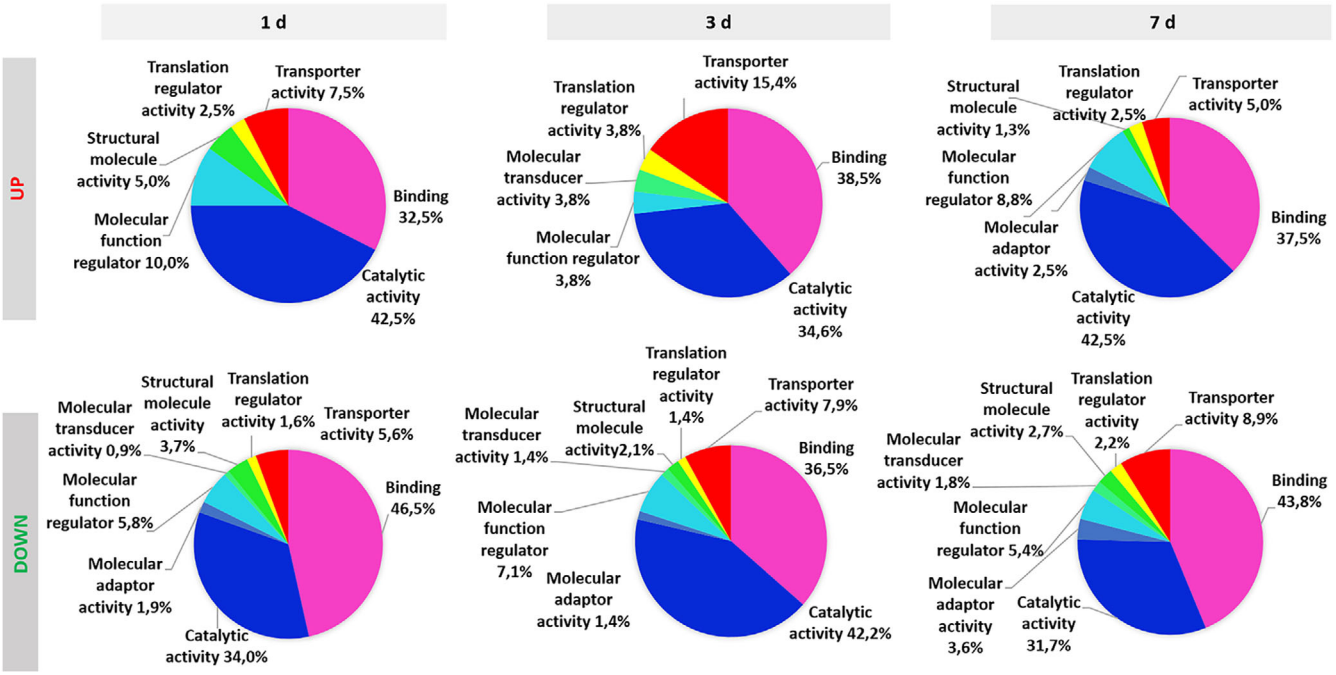

FIGURE 1 PANTHER pie charts of molecular functions associated with the proteins differentially expressed in HOb cells cultured on SAE-Ti compared to those cultured on C

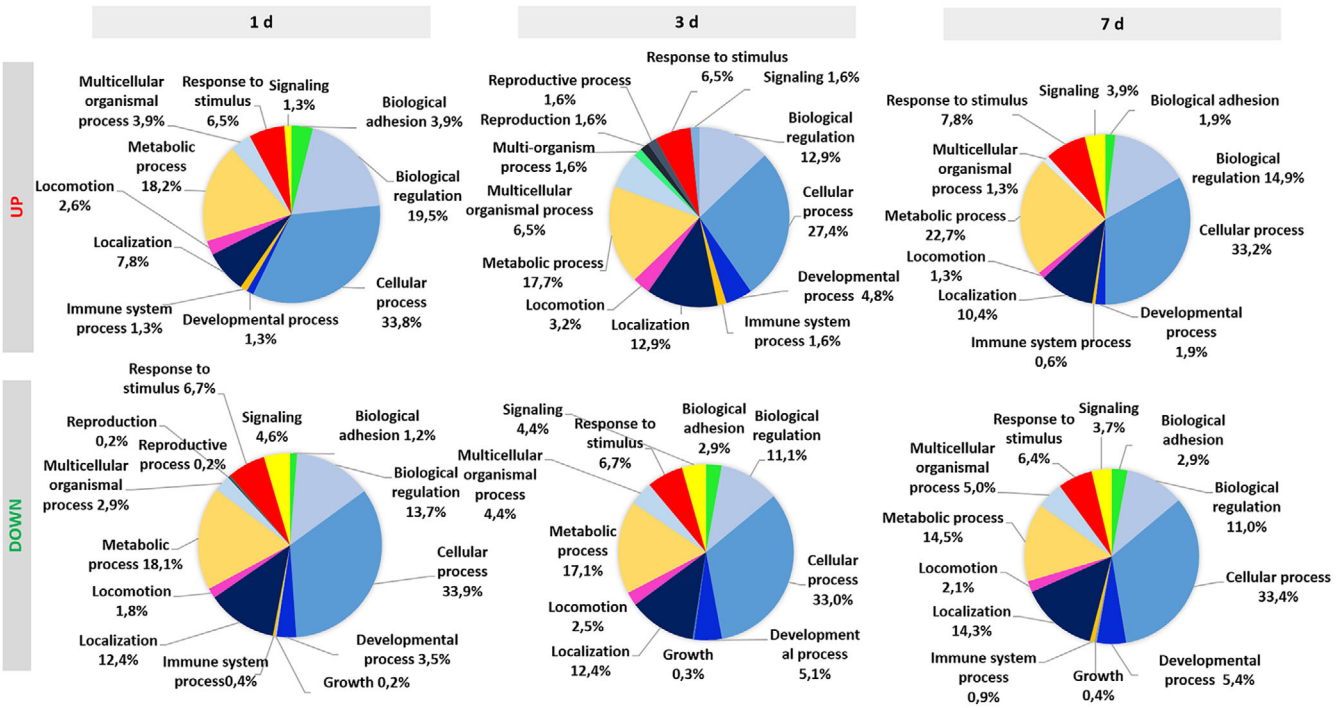

FIGURE 2 PANTHER pie charts of biological functions associated with the proteins differentially expressed (upregulated or downregulated) in HOb cells cultured on SAE-Ti compared to the C cells

molecular and biological functions associated with the proteins differentially expressed by HOb cells cultured on SAE-Ti (compared with C) are shown in Figures 1 and 2. The PANTHER pie charts of molecular functions showed that most of the differentially expressed proteins were mainly related to catalytic activity, binding and transporter activity. To a lesser extent, both downregulated and upregulated proteins, at all the examined time points, were associated with the regulation of molecular functions and translation activity. Between 2% and 4% of

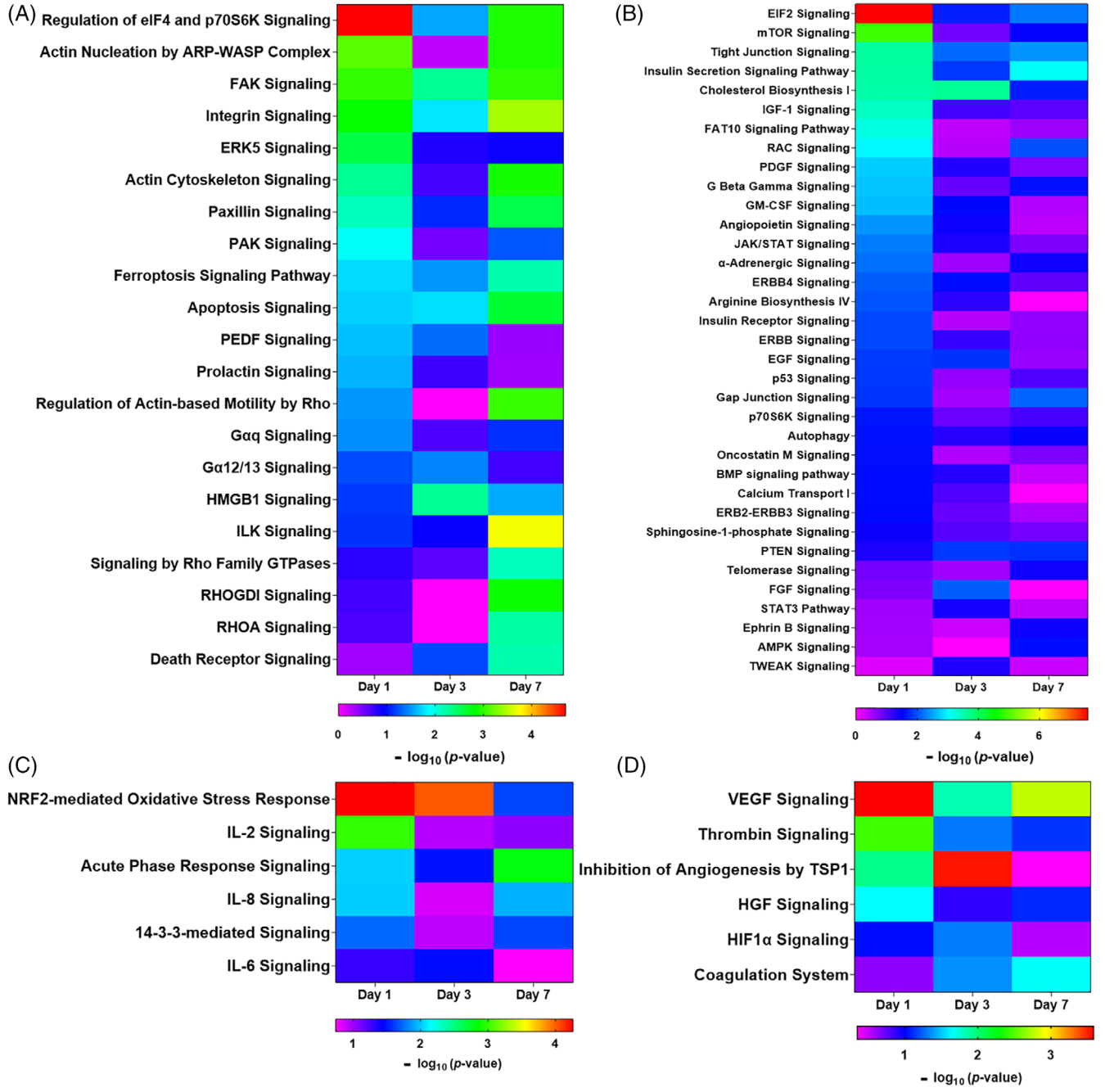

FIGURE 3 Distribution of enriched pathways obtained in IPA analysis. The statistical functional enrichment of the canonical pathways for the differentially expressed proteins (SAE-Ti vs. C) is shown in terms of −log (*p*-value). *p*-values show the probability that the association between a set of proteins and a given pathway is due to random chance (right-tailed Fisher's exact test). A pathway is considered statistically enriched for −log (*p*-value) > 1.3, which is obtained for *p*-value <.05. Identified pathways were classified into four functional categories: (A) adhesion and proliferation, (B) osteogenesis, (C) immunity and oxidative stress, and (D) coagulation and angiogenesis

downregulated proteins were associated with structural molecule activity functions; 5% of the upregulated proteins were associated with these functions after 1 day and 0% and 1.3% after 3 and 7 days of culture, respectively. Likewise, the molecular transducer and molecular adaptor activities were identified for the proteins downregulated over time. In contrast, for the upregulated proteins, the molecular transducer activity only appeared at 3 days and the molecular adaptor activity at 7 days of incubation.

Figure 2 shows the PANTHER pie charts of biological functions for differentially expressed proteins throughout the culture time. In this ranking, the most prominent biological functions for the studied conditions were related to the cellular and metabolic processes, biological regulation, localisation and response to a stimulus. To a lesser extent, proteins associated with the multicellular organismal process, locomotion, signaling and developmental process were also identified. Upregulated proteins associated with biological adhesion were

detected (3.9%) after 1 day; their contribution changed to 0% and 1.9% after 3 and 7 days, respectively. Among the downregulated proteins, the biological adhesion function was associated with 1.2% of the proteins after 1 day, increasing to 2.9% after longer culture periods. Immune system process functions were associated with 0.4%–1.6% of the proteins (except for downregulated proteins at 3 days). Some biological functions were only detected for a small proportion of the differential proteins under specific experimental conditions. For example, the reproduction and reproductive process functions were associated with 0.24% of the downregulated proteins at 1 day and 1.6% of the upregulated proteins after 3 days. Growth functions were only detected for the downregulated proteins, and multi-organism process functions were only associated with the upregulated proteins detected after 3 days.

3.2.2 | IPA relative functional analysis

The IPA bioinformatics tools were used to obtain the pathways enriched in the detected differentially expressed proteins (SAE-Ti vs. C) at 1, 3, and 7 days (Figure 3). Sixty-eight pathways were identified and classified within four possible sets: adhesion and proliferation, osteogenesis, immunity and oxidative stress, and coagulation and angiogenesis. On day 1, the pathways with the highest activity were the EIF2 signaling and mTOR signaling, both related to osteogenic functions. In fact, these osteogenic signals at day 1 displayed the highest −log(*p*-value) among the results for the three examined time points. A large proportion of the enriched pathways were associated with osteogenesis (35 of 68). The regulation of eIF4 and p70S6K signaling, associated with cell adhesion processes, took third place among the enriched pathways. Twenty-one of the detected pathways were classified within the group of adhesion and proliferation, the second most represented set of pathways in the results. Only six pathways were associated with immunity and oxidative stress and another six with coagulation and angiogenesis. Pathway enrichment varied with culture duration; generally, the −log(*p*-value) values and the number of statistically enriched pathways tended to decrease over time.

The IPA Molecule Activity Predictor tool predicted the upstream molecules related to the differentially expressed proteins examined in the SAE-Ti versus C comparisons (Table S3). Among the molecules predicted as activated on day 1, there should be the sirolimus, RICTOR and torin-1 molecules, which play a pivotal role in the mTOR signaling pathway. In Figure 4, the relationships that allowed IPA to predict the activation of RICTOR are shown as an example. The differential activation (SAE-Ti vs. C) of COL5A1 and MAP4K4 was also foreseen for day 1. Significant activation of RUNX2, WNT3A and COL5A1 proteins (with key functions in osteogenesis) was predicted for a prolonged culture with SAE-Ti.

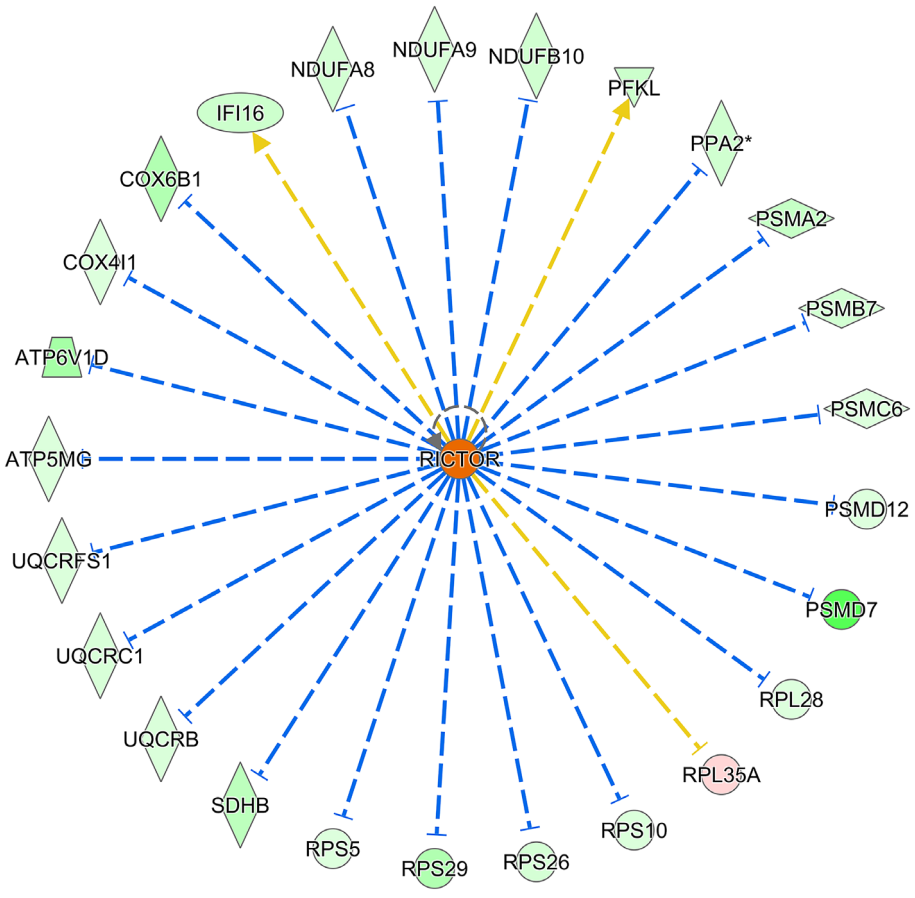

FIGURE 4 RICTOR activation prediction by IPA Upstream Regulator tool (at day 1). Blue lines show the predicted relationships leading to inhibition, and yellow lines, the inconsistent findings. Downregulated proteins are displayed in green and upregulated in pink. The figure shows that the reduced expression of a group of proteins associated with the inhibition of RICTOR allows the IPA software to predict the presence of this molecule

3.3 | Functional classification of SAE-Ti differential proteins over time

3.3.1 | PANTHER classification

The PANTHER analysis of proteins differentially expressed in HOb cells cultured on SAE-Ti for different periods is displayed in Figure 5. Binding, catalytic activities, molecular function regulation, transporter, structural molecule, molecular adaptor, and translation regulator activities were the molecular functions detected for the proteins with levels of expression altered after 3 and 7 days compared to day 1 of culture. The proportion of proteins related to catalytic activity functions increased with the incubation time to 47.6% of the upregulated proteins after 7 days. Differentially upregulated proteins (in comparison with day 1) with transporter activity functions reached 7.7% and 6.0% after 3 and 7 days of culture, respectively. In this analysis, the differentially downregulated proteins were those more abundant on day 1 than after 3 and 7 days. The levels of proteins with transporter activity functions at day 1 were lower (2.3% and 3.2% for 3 days vs. 1 day and 7 days vs. 1 day, respectively). In contrast, the number of differential proteins associated with binding functions tended to decrease with time. Thus, in the comparison between 3 and 1 day, this molecular function was linked with 40.2% of the proteins more abundant at day 1 (downregulated on day 3) and 36.5% of the proteins upregulated after 3 days. These slight differences became more significant after 7 days of culture, reaching 45.4% for the downregulated and 29.8% for the upregulated proteins.

Several biological functions were associated with the proteins whose expression was altered after 3 and 7 days of culture. These were the cellular, immune system and developmental processes, localisation, locomotion, metabolic and multicellular organismal processes, response to stimulus, signaling, biological adhesion and biological regulation functions (both for upregulated and downregulated proteins). The number of proteins associated with developmental and multicellular organismal processes and response to stimulus increased after 3 days of culture. The reproduction and reproductive process (0.6%) were only associated with proteins downregulated after 7 days (compared to day 1); these functions were linked to differential proteins with levels higher at day 1 than at 7 days of incubation. Likewise, the growth function was identified only for the proteins expressed in larger amounts on day 1 than after 3 days.

3.3.2 | DAVID analysis

DAVID enrichment analysis was employed to identify clustering annotation groups for proteins differentially expressed in HOb cells cultured on SAE-Ti for different periods. The changes in the linked functions during this period and the related proteins are shown in Table S4. A large number of proteins were associated with adhesion. Among the proteins upregulated after 3 days (in comparison with 1-day culture), only seven were related to focal adhesion (GO:0005925) functions. In contrast, 27 downregulated proteins were associated with focal adhesion, cell–cell adhesion (GO:0098609), cell–cell adherens junction (GO:0005913) and cadherin binding involved in cell–cell adhesion (GO:0098641). After 7 days, these differences increased; 96 proteins whose expression was reduced in comparison with day 1 were associated with cell–cell adhesion, cadherin binding involved in cell–cell adhesion, cell–cell adherens junction, actin filament binding (GO:0051015), and cell adhesion (GO:0007155) processes. Although fewer overexpressed adhesion-associated proteins were detected after 7 days (in comparison with 1-day culture), they were also related to functions in focal adhesion, cell adhesion, actin binding (GO:0003779), cell–cell adhesion, cadherin binding involved in cell–cell adhesion, and cell–cell adherens junction. In the cluster related to coagulation and angiogenesis, the upregulated and downregulated proteins with functions in platelet activation (GO:0030168) and angiogenesis (GO:0001525) were detected in both comparisons. Enrichment in functions related to immunity and oxidative stress was also observed. The proteins upregulated after 3 and 7 days (in comparison with 1-day incubation) linked to these functions were associated with the regulation of immune response (GO:0050776). However, among the proteins at higher levels after 1 day of culture than after 3 days (DOWN condition), oxidation–reduction process (GO:0055114), oxidoreductase activity (GO:0016491), positive regulation of NF-kappaB transcription factor activity (GO:0051092), and innate immune response (GO:0045087) functions were enriched. In the proteome profile obtained after 7 days of culture (compared to day 1), the proteins linked to NIK/NF-kappaB signaling (GO:0038061), tumor necrosis factor-mediated signaling pathway (GO:0033209), and T cell receptor signaling pathway (GO:0050852) functions were downregulated. Among the osteogenic functions, the proteins with levels increased at 3 and 7 days of culture were related to the positive regulation of protein kinase B signaling (GO:0051897), insulin-like growth factor binding (GO:0016942), and MAPK cascade (GO:0000165). There were no clusters of proteins enriched in osteogenic functions in the downregulated group (3 days vs. 1-day comparison). However, the comparison of 7-day and 1-day cultures identified proteins with functions in the positive and negative regulation of canonical Wnt signaling pathway (GO:0090263 and GO:0090090) and MAPK cascade and insulin receptor signaling pathway (GO:0008286). Moreover, a cluster of functions with a key role in the extracellular matrix formation was also found. Among the downregulated proteins, those related to collagen fibril organization (GO:0030199) and extracellular matrix organization (GO:0030198) were only detected in the 7-day versus 1-day comparison. For the proteins with expression increased after 3 and 7 days, the extracellular matrix (GO:0031012), collagen fibril and extracellular matrix organization functions were enriched. Moreover, the upregulated proteins COL1A1, COL3A1, HAPLN1, COL1A2, COL2A1, AHSG, RBP4, EPHA2, SULF1, COL11A1, COL12A1, IGF2, and COMP were directly related to the skeletal system development (GO:0001501).

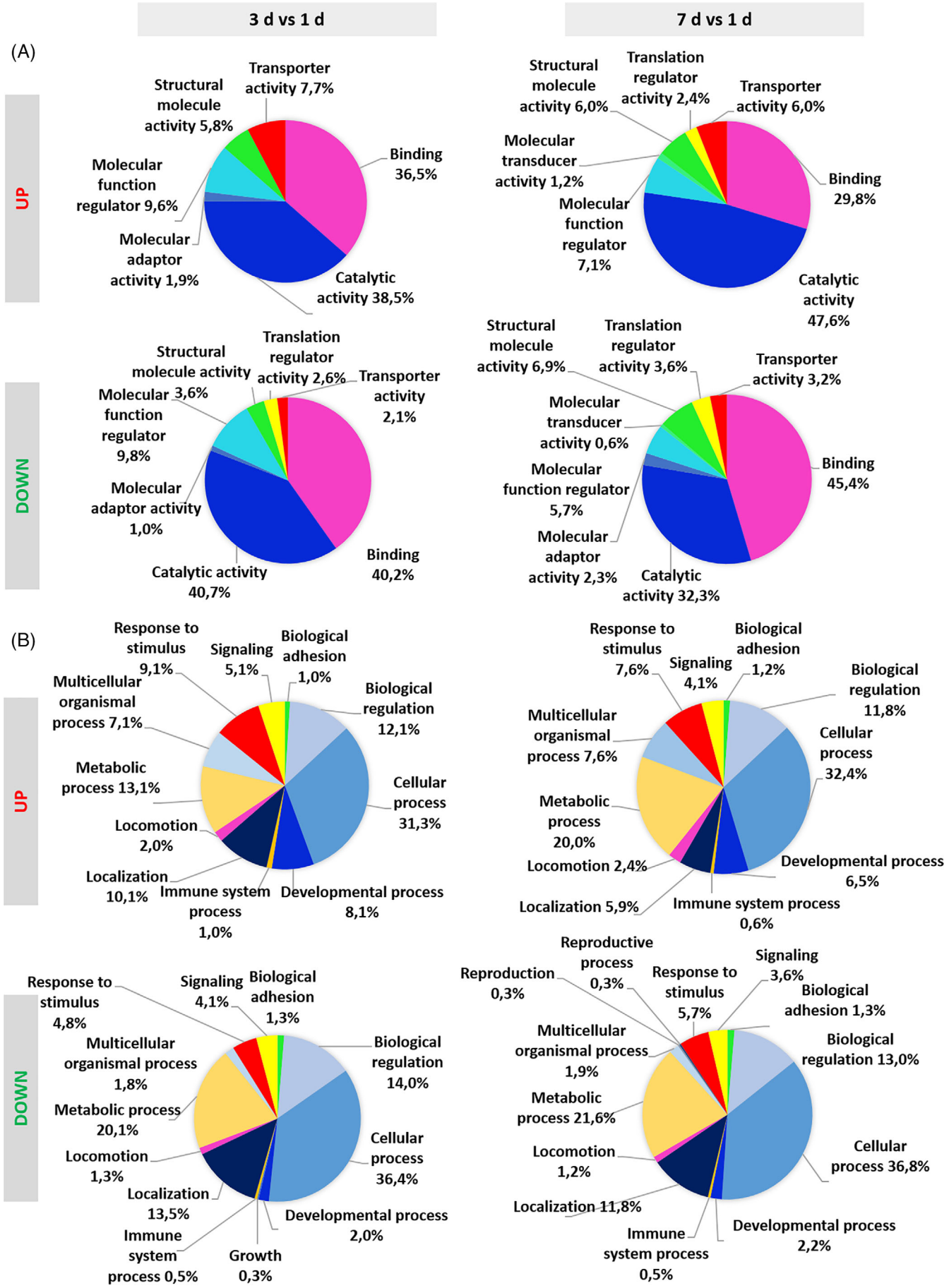

FIGURE 5 Legend on next page.

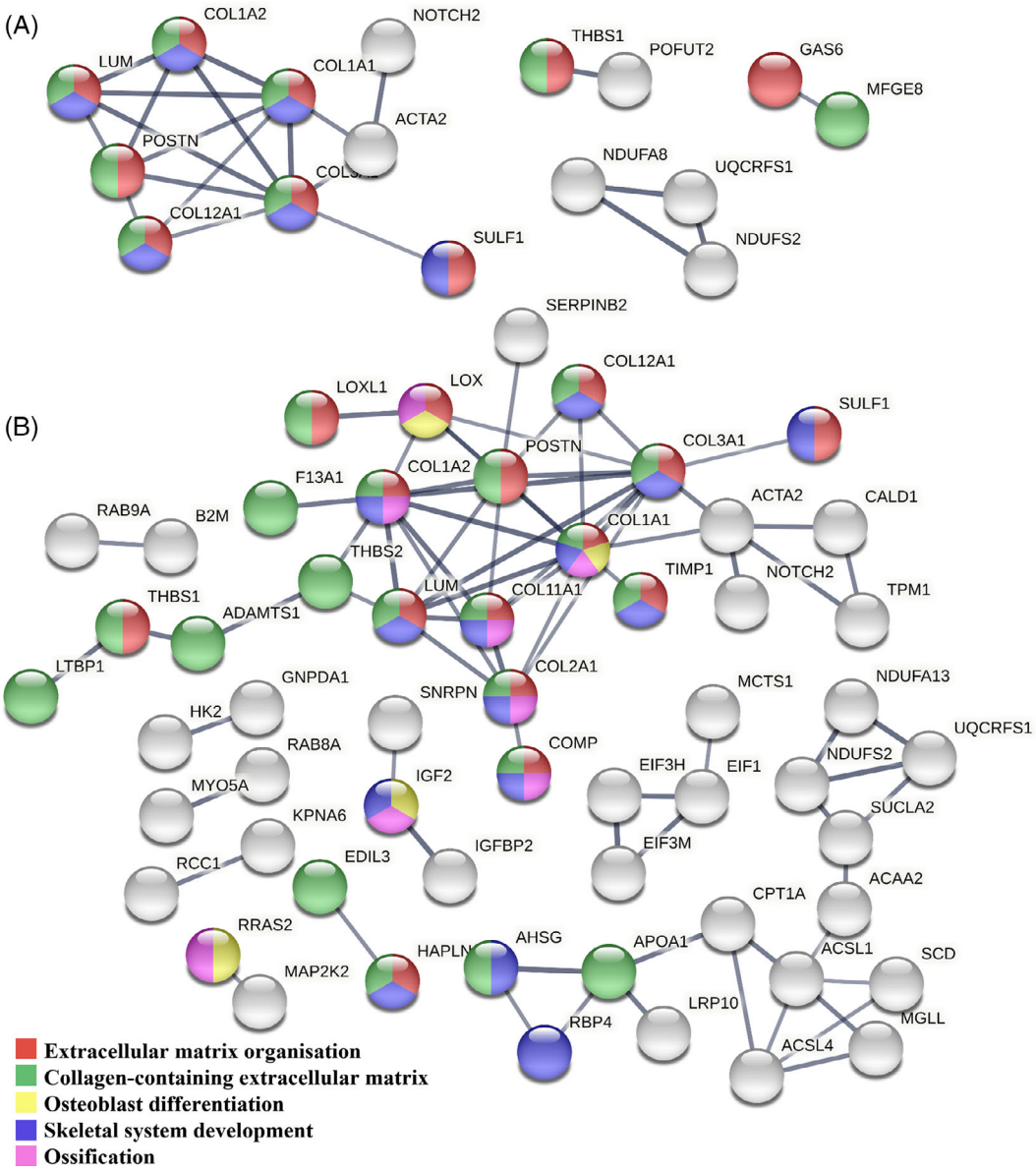

FIGURE 6 STRING interaction networks between upregulated differential proteins in HOb cells cultured for (A) 3 days and (B) 7 days in comparison with the proteome expression at day 1. Line thickness indicates the interaction strength. Proteins are indicated using their gene names. Colors are related to the protein functional classification: extracellular matrix organization (red), collagen-containing extracellular matrix (green), osteoblast differentiation (yellow), skeletal system development (blue), and ossification (purple)

3.3.3 | Protein network visualizations

Interaction networks for differentially upregulated HOb proteins over time were obtained using STRING software. The identified relationships are shown in Figure 6. The proteins in the networks were also related to the extracellular matrix organization, osteoblast differentiation, skeletal system development and ossification functions, as well as to be a collagen-containing extracellular matrix protein-type.

3.4 | In vitro experiments

To evaluate their osteogenic potential, the SAE-Ti and C materials were used in in vitro cultures of HOb cells (Figure 7). The capability of osteoblasts to proliferate on SAE-Ti and C materials is illustrated in Figure 7A. The proliferation was reduced on the Ti surface after 7 days of culture. To examine mineralization, the ARS staining was employed to measure the formation of calcium-rich deposits

FIGURE 5 PANTHER pie charts of (A) molecular and (B) biological functions associated with the proteins (UP/DOWN) differentially expressed on HOb cells cultured on SAE-Ti for 3 and 7 days, compared to 1-day culture

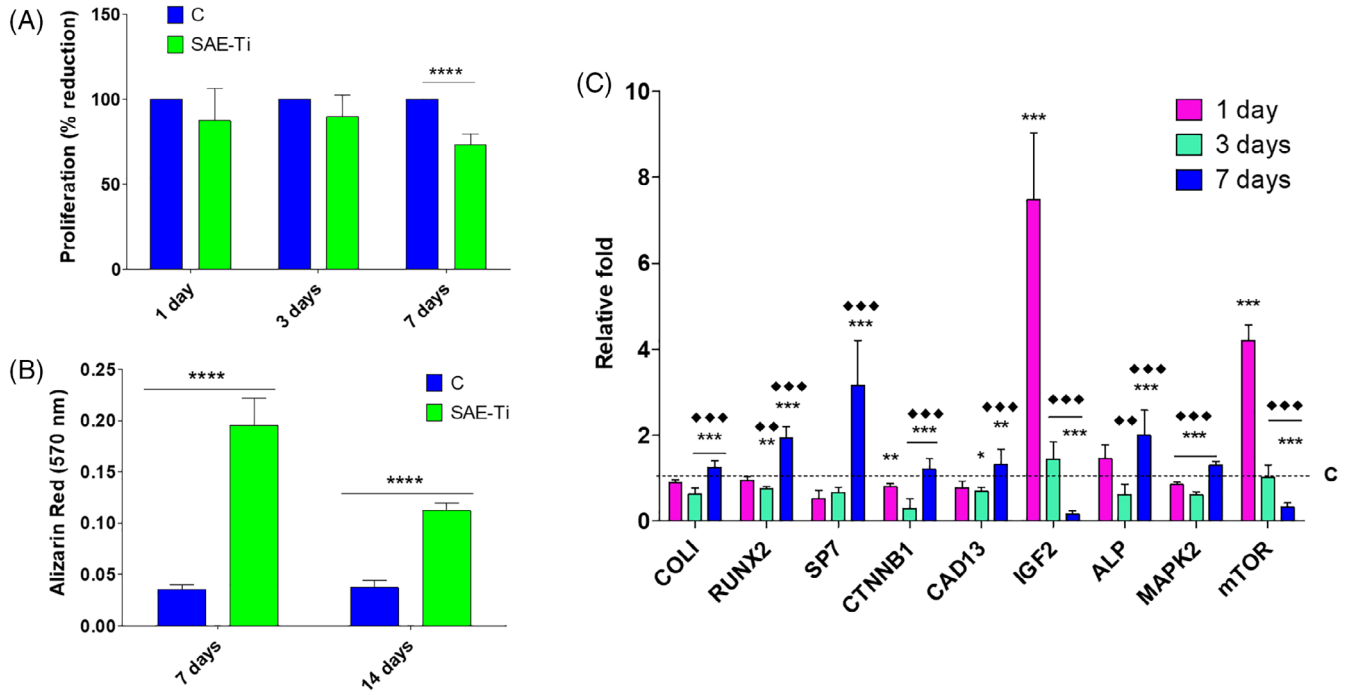

FIGURE 7 HOb in vitro culture results: (A) cell proliferation measurements at 1, 3, and 7 days using MTS ($n = 3$); (B) mineralization capability measured by Alizarin Red staining at 7 and 14 days ($n = 3$); (C) relative expression of target genes after 1, 3, and 7 days of culture measured by qRT-PCR ($n = 4$). The assessed target genes were collagen I (COLI), runt-related transcription factor 2 (RUNX2), transcription factor SP7/osterix (SP7), β-catenin (CTNNB1), cadherin-13 (CAD13), insulin growth factor 2 (IGF2), alkaline phosphatase (ALP), MAPK Activated Protein Kinase 2 (MAPK2), and mechanistic target of rapamycin (mTOR). Data were normalized to control (C; wells without SAE-Ti) using the $2^{-\Delta\Delta Ct}$ method. Results are shown as mean ± SE

produced by HOb cells grown on these materials (Figure 7B). The SAE-Ti samples showed increased mineralization compared to C after 7 and 14 days of culture. Figure 7C displays the gene expression results. The expression of collagen I (COLI) and runt-related transcription factor 2 (RUNX2) rose after 7 days of culture with SAE-Ti in comparison with C. It was detected that the expression of these genes was lower after 3 days than on day 1 but higher after 7 days. The expression of the transcription factor SP7 (SP7) gene significantly increased on SAE-Ti compared with C after 7 days. Moreover, the SP7 expression on SAE-Ti after 7 days was higher than on day 1. The expression of β-catenin (CTNNB1) on SAE-Ti after 1 and 3 days was lower than on C; after 7 days, it was higher for SAE-Ti. CTNNB1 expression on SAE-Ti changed during the examined period; it dropped after 3 days and increased after 7 days. Similarly, the expression of cadherin-13 (CAD13) on SAE-Ti compared to C diminished at 3 days and increased after 7 days. On SAE-Ti, it was higher at 7 days than on day 1. The insulin growth factor 2 (IGF2) and mechanistic target of rapamycin (mTOR) expression significantly increased on SAE-Ti compared to C after 1 day of culture and decreased after 7 days. Regarding the evolution of the expression of these two genes on SAE-Ti over time, both markers decreased with time; they were lower after 3 and 7 days than on day 1. The expression of alkaline phosphatase (ALP) in SAE-Ti (compared to C) only increased after 7 days of culture. The cells cultured with SAE-Ti reduced their expression of ALP after 3 days in comparison with day 1. However, they increased it again after 7 days. MAPK Activated Protein Kinase 2 (MAPK2) showed a significantly elevated expression on C at 1 and 3 days, while after 7 days of culture, it was higher on SAE-Ti. The MAPK2 expression reduced at 3 days and increased after 7 days on SAE-Ti, in comparison with day 1.

4 | DISCUSSION

Proteomic analysis of cellular molecular profiles offers effective methods to overcome the limitations of traditional in vitro characterization of biomaterials. It can also improve our understanding of the biology of regeneration processes. Here, we characterized the proteome of HOb cells cultured on SAE-Ti for 1, 3, and 7 days. The physicochemical properties, surface adsorption patterns of serum proteins, osteogenic potential in vitro and the in vivo osseointegration properties of SAE-Ti implants have been described before.[21,24,25]

In the first step, the proteomic profiles of cells incubated with SAE-Ti and those grown in empty polystyrene wells (C; routinely used as controls in in vitro testing) were compared to identify the cellular mechanisms associated with exposure to SAE-Ti. A large number of proteins were identified, 2544 in total. Moreover, important differences were detected between protein expression levels in SAE-Ti and C samples. These results reflect the different material–cell interactions that condition protein expression in the osteoblasts in response

to changes in their environment.[18] The differentially expressed proteins were then classified according to their function using PANTHER. Our relative functional analysis of the protein expression profiles on SAE-Ti and C (using the IPA tools) revealed 68 enriched pathways related to the regeneration process. Most of these pathways were associated with the adhesion, proliferation and differentiation of osteoblasts. Moreover, the pathways linked to coagulation, angiogenesis, immunity and oxidative stress were also found more active. Osteoblast adhesion and spreading occur in the first stage of tissue regeneration in the vicinity of implants. These processes are mediated by different proteins such as integrins, cytoskeletal proteins, cell membrane proteins, extracellular matrix proteins, and cadherins.[26] The interaction of osteoblasts with a biomaterial can modify the expression of these proteins, depending on the properties of the material[27]; this was also demonstrated in the current study. Moreover, it seems that the adhesion mechanisms of osteoblasts grown on SAE-TI and C not only differ at the level of integrin activity but also in their cell–ECM mediation signaling. The activity of pathways involved in forming focal adhesions, such as integrin, integrin-linked kinase (ILK), focal adhesion kinase (FAK), and Rho-family signaling, were found as altered. The IPA analysis of osteogenic pathways revealed that the eukaryotic initiation factor 2 (EIF2) and the mechanistic target of rapamycin (mTOR) signaling were the pathways with differentially increased activity as a consequence of changes in specific protein expression. Ge et al.[28] have characterized the MC3T3 osteoblast-derived exosomes by mass spectrometry; they have found that the identified osteogenesis-related proteins were associated with an important activity in the EIF2 pathway. The regulation of eukaryotic proteins occurs mostly during translation initiation, controlled by eukaryotic initiation factor proteins (EIFs). These proteins are required for the assembly of a translationally competent 80S ribosome, needed for the elongation and subsequent polypeptide synthesis.[29] The process involves phosphorylation of the α subunit of EIF2 (eIF2α∼P), which represses the initiation phase of protein synthesis, allowing cells to conserve resources while a new gene expression programme is adopted to prevent stress damage[29,30] EIF1, EIF3M, EIF5A, and GCN1, which facilitate the formation of the eIF2α-P complex,[31] were upregulated in SAE-Ti samples. However, the EIF2S3, EIF2S2, EIF2A, EIF3A, EIF3A, EIF4G2, and EIF4G3 were differentially downregulated in the cells exposed to SAE-Ti. This pathway could be involved in the cellular response at the translation level, countering the stress caused by the exposure to the tested materials. The EIF2 signaling pathway is related to osteoblast differentiation and bone formation.[28] Hamamura et al.[32] have suggested that an increase in EIF2A phosphorylation not only stimulates osteoblastogenesis but also can inhibit osteoclastogenesis. Although the role of mTOR in bone processes is not fully understood, and reports are sometimes providing contradictory information,[33] it is clear that this pathway affects the osteogenic process.[34] Pantovic et al.[35] have found that the AMP-activated protein kinase (AMPK) controls osteogenic differentiation of hMSCs via early mTOR inhibition-mediated autophagy and late activation of AKT/mTOR signaling. Curiously, our IPA analysis found that both the AMPK activity and autophagy were increased by culturing the cells in the presence of SAE-Ti. mTOR can regulate IGF signaling (also altered in such cultures) by phosphorylation of IGF2 mRNA-binding proteins (IGF2BP), thus increasing IGF2 production.[36] The IGF2 expression was significantly higher in SAE-Ti samples than in C cultures after 1 and 3 days but decreased after 7 days. Its pattern was similar to the mTOR expression profile in these samples. The proteomic analysis showed a decrease in the level of IGF2BP2 (2-fold) at day 1 and an increase in the level of IGF2 (3-fold) after 7 days on SAE-Ti in comparison with controls. This observation might indicate an involvement of mTOR/IGF signaling in the osteogenic response to Ti. The mTOR signaling can be activated by two different protein complexes: mTORC1 and mTORC2. Moreover, the RAPTOR and RICTOR components are essential for forming mTORC1 and mTORC2 multiprotein complexes, respectively.[34] We found an increase in the activity of this signaling pathway. This observation was supported by the increased mTOR gene expression after 1 day of culturing with SAE-Ti. The analysis of upstream regulators predicted the RICTOR and sirolimus (rapamycin) activation and RAPTOR inhibition. This is consistent with the observed reduction in LAMTOR3 expression in cells cultured with SAE-Ti for 1 day; LAMTOR3 protein is a part of Ragulator complex involved in mTORC1 activation.[36] Moreover, although rapamycin inhibits mTORC1, it has no effect on mTORC2.[37] Therefore, it is possible that SAE-Ti and C materials trigger different mechanisms to activate this mTOR pathway. The activity detected in SAE-Ti cultures could be associated with a differential activation of *mTORC2*. mTORC2 can be activated by growth factors such as insulin/IGF or Wnt, as well as by mechanical stress.[34] Rough titanium surfaces, such as SAE, can alter the local mechanical environment,[38] which could also explain the obtained results. Generally, mTORC2 is linked to cell proliferation and survival, while mTORC1 is the complex usually associated with the osteoblastic differentiation. However, some studies suggest that the activation/inhibition kinetics of the pathway is the key to the correct skeletal development, as mTORC2 is also necessary for optimal skeletal growth and bone anabolism.[33,38] Ours results support this idea, as SAE-Ti samples show an increased mineralization and an elevated expression of osteogenic genes involved in the differentiation potential of osteoblasts. The differential protein expression in SAE-Ti samples associated with this pathway highlights its potential importance in the bone regeneration process in tissues close to an implant. We also observed increased activity in coagulation-related pathways; the expression of proteins associated with the coagulation cascade was upregulated in cells cultured on SAE-Ti. Factor X protein levels increased 20-fold in SAE-Ti samples after 1 day of culture and 30-fold after 7 days (the second most upregulated protein). The expression of AHSG and factor XIIIA proteins also increased (15- and 7-fold, respectively) in osteoblasts in contact with SAE-Ti. It has been reported that the expression and secretion of factor XIIIA by MC3T3-E1 cells is required for osteoblast COL1 secretion and extracellular deposition, and thus also for osteoblast differentiation.[39]

Moreover, the protein expression in HObs cultured with SAE-Ti changes over time, reflecting the processes involved in cell adhesion, proliferation and differentiation on this biomaterial. In general, a decrease in the number of HOb-expressed proteins with functions

associated with adhesion from day 1 of incubation was found. The expression of proteins associated with the oxidation–reduction and immune response processes also decreased with the increasing time of culture. Moreover, the group of overexpressed proteins associated with this cluster of functions was formed mainly by collagens (COL2A1, COL3A1, COL1A1, and COL1A2), which were linked to the regulation of this response. The changes in these inflammatory processes can be correlated with the initial pro-inflammatory response to Ti implants. Indeed, the complement system proteins have been detected in the protein layer deposited onto Ti surfaces; these are the proteins that can affect osteoblast responses and increase osteogenesis by osteoimmune modulation.[21,25] The expression of pro-inflammatory proteins by MG-63 osteoblasts have also been reported in a proteome study using inert biomaterials.[18] The decrease in the expression of these pro-inflammatory proteins observed from the first day of culture could reflect a rapid adaptive response of the cells to the SAE-Ti material. Among the proteins related to platelet activation and angiogenesis, it is remarkable the increased expression over time in HOb cultured with SAE-Ti of thrombospondin-family proteins THBS1, THBS2, THBS4, and COMP (thrombospondin-5). THBS1 is considered a potent inhibitor of angiogenesis, as well as a regulator of inflammation and an inhibitor of T cell and dendritic cell activation.[40] THBS2 and THBS4 are associated with increased angiogenesis, in part due to altered endothelial cell–ECM interactions.[41,42] Moreover, the proteins from this family are associated with the ECM organization and creation; they participate in ECM assembly, cell–ECM interactions and tissue remodeling during the response to injury.[41–43] This is consistent with the results of the DAVID analysis conducted in our study; the expression of proteins related to ECM and collagen organization increased during the incubation with SAE-Ti. Bone ECM plays a key role during implant osseointegration as it can induce the production of new bone by osteoblast-lineage cells. Collagens type I, III, and V are the most abundant constituents of the organic ECM in bones; COL1 constitutes 90% of the total collagen in bone tissue.[44,45] Here, the COL2A1, COL3A1, COL11A1, COL12A1, COL1A1, and COL1A2 were among proteins overexpressed in SAE-Ti cultures. Exposure to SAE-Ti resulted in increased gene expression of COL1 after 7 days of in vitro culture compared to controls. Moreover, the expression of COL1 increased with the time of incubation with SAE-Ti (up to 7 days), which was consistent with the proteomic results. Collagen acts as a tissue scaffold, forming a matrix for anchoring cells and regulating the growth and osteogenic properties of osteoblasts.[44] COL1 can induce differentiation of bone marrow cells, leading to increased expression of ALP, OCN, and BSP.[46] DAVID analysis revealed an enrichment in the positive regulation of protein kinase B signaling, insulin-like growth factor signaling and MAPK cascade with the incubation time. Among the osteogenic proteins whose expression continued to rise during the 7-day culture, the RBP4, IGF2, and GAS6 were also more abundant in the proteome profile of cells exposed to SAE-Ti than in the profile of control cells (C). RBP4 was the protein with the largest increase in its expression after the exposure to SAE-Ti (114-fold after 7 days). The overexpression of RBP4 has been associated with increased proliferation, differentiation and mineralization in MC3T3-E1 murine cell line. Moreover, the expression of RUNX2, OC, OPN, and COL1 genes were considerably elevated in RBP4-overexpressed MC3T3-E1 cells.[47] Among the proteins involved in the IGF signaling, IGFBP2 and IGF2 increased their expression during the experiment. For IGFBP2, an 8-fold increase was observed, and the IGF2 expression rose 2-fold after 3 days and 4-fold after 7 days. The qRT-PCR analysis also showed an elevated expression of the IGF2 gene in SAE-Ti samples after 3 and 7 days of culture. The IGF2 potentiates the osteogenic differentiation and augments BMP-9-induced bone formation.[48] The growth arrest-specific protein 6 (GAS6) is associated with the activation of phosphatidylinositol 3-kinase (PI3K), extracellular signal-regulated kinase (ERK), and nuclear factor kappa-light-chain-enhancer of activated B cells (NF-κB) pathways. This protein is involved in adjusting the cellular processes of apoptosis, survival, proliferation, migration and adhesion.[49] The extracellular matrix protein TNC, which was also differentially upregulated during the culture time with SAE-Ti, can be expressed by osteoblasts from the onset of ossification and continues to do so in growing bone. It can stimulate osteoblastic differentiation and help to maintain osteoblast functionality. The inhibition of TNC provokes a reduction in ALP levels and reduces collagen synthesis in osteoblastic cells.[50] Kidwai et al.[51] have reported high FGF1 levels in neural crest-derived osteogenic progenitors. Their study has demonstrated that FGF1 affects RUNX2 levels, with concomitant changes in ERK1/2 signaling. Here, the FGF1 was also one of the osteogenic proteins whose expression rose in the HOb cultures exposed to SAE-Ti over time. Another overexpressed protein, MAP2K2 (3-fold increase after 7 days), can activate the ERK MAPK pathway. This promotes osteoblast differentiation and bone formation in vitro and in vivo via control of osteoblast master regulators, including RUNX2, ATF4, and β-catenin.[52] EPHA2 protein (here, the 4-fold increase observed after 7 days) has been identified as a major MAPK activator in exosomes.[53] The EPHA2 also can reduce the apoptosis of epithelial cells by inhibiting autophagy via activating PI3K/Akt/mTOR pathway.[54] The changes in protein expression with the time of culture of the cells in contact with SAE-Ti can be correlated with the osteogenic response to this material in vitro. The expression of ALP, RUNX2, SP7, CTNNB1 (β-catenin), CAD13, and MAPK2 increased throughout the 7-day culture with SAE-Ti; the expression levels of these genes were also higher in cells in contact with this material than in C samples.

In addition to identifying enrichment in functions associated with the ECM and osteogenesis, key for implant osseointegration, DAVID analysis detected a protein cluster associated with the development of the skeletal system, containing the proteins whose expression increased in the HOb cells cultured on SAE-Ti. COL1A1, COL3A1, HAPLN1, COL1A2, COL2A1, AHSG, RBP4, EPHA2, SULF1, COL11A1, COL12A1, IGF2, and COMP were included in this cluster. These results were supported by an additional study using the Search Tool for the Retrieval of Interacting Genes/Proteins (STRING). The STRING analysis produced protein networks with upregulated differential proteins in HOb cells cultured for 3 and 7 days in comparison with the proteome expression at day 1. After 3 days of culture, the principal network was mainly composed of proteins associated with

ECM organization and skeletal system development. After 7 days, the osteoblast differentiation and ossification processes were also detected, essential for bone regeneration around an implant.

Identifying proteins with key functions in the regenerative processes whose expression changes over time in osteoblasts cultured on SAE-Ti, and detecting the characteristic cellular mechanisms triggered by exposure to this material will help improve our understanding of the osseointegration process.

5 | CONCLUSION

Detailed studies of the effects of biomaterials on the osteoblast-related regenerative mechanisms are important for understanding the bone healing process around implants. The proteomic characterization of the impact of exposing the HOb cells to SAE-Ti revealed that most of altered pathways by the presence of the SAE-Ti samples on the culture wells were related to osteoblast adhesion, proliferation, and differentiation; all them important in bone tissue regeneration around the implant. Our proteomic results showed that SAE-Ti not only affects integrin activation (via pathways such as integrin, ILK, FAK or Rho-family signaling) but also the mediation signaling between the cell and the ECM, as well as, EIF2, mTOR, and IGF, with important functions in osteoblast proliferation and differentiation. The comparison of proteomic profiles obtained for SAE-Ti samples after distinct incubation periods allowed identifying the changes in cellular mechanisms over time caused by the HOb exposure to this biomaterial. Among the proteins, differentially upregulated over time, a cluster of proteins related to the development of the skeletal system was identified. The increased expression of thrombospondins, collagens, RBP4, IGF2, GAS6, TNC, MAP2K2, FGF1, and EPHA2, with key roles in the osteogenesis and ECM formation can explain the SAE-Ti-related osteogenesis. These results showed the global impact of Ti on HOb cells, improving our knowledge of the effects of this material on the cellular mechanisms.

ACKNOWLEDGMENTS

The work was supported by Ministerio Ciencia e Innovación (PID2020-113092RB-C21); Generalitat Valenciana (APOSTD/2020/036 and PROMETEO/2020/069); Universitat Jaume I (UJI-B2021-25); and the University of the Basque Country (GIU18/189). The authors would like to thank Raquel Oliver, Jose Ortega, and Iraide Escobés for their valuable technical assistance, and the company GMI-Ilerimplant for producing the titanium discs.

CONFLICT OF INTEREST

The authors declare no potential conflict of interest.

DATA AVAILABILITY STATEMENT

The data underlying this article will be shared on reasonable request to the corresponding author. The mass spectrometry proteomics data have been deposited to the ProteomeXchange Consortium via the PRIDE partner repository with the dataset identifier PXD035986.

ORCID

Francisco Romero-Gavilán https://orcid.org/0000-0001-8300-7248
Andreia Cerqueira https://orcid.org/0000-0001-9281-069X

REFERENCES

1. Brånemark PI, Hansson BO, Adell R, et al. Osseointegrated implants in the treatment of the edentulous jaw. Experience from a 10-year period. *Scand J Plast Reconstr Surg Suppl*. 1977;16:1-132.
2. Hanawa T. Titanium-tissue interface reaction and its control with surface treatment. *Front Bioeng Biotechnol*. 2019;7:170.
3. Williams DF. Titanium for medical applications. In: Brunette DM, Tengvall P, Textor M, Thomsen P, eds. *Titan Med Mater Sci Surf Sci Eng Biol Responses Med Appl*. Springer; 2001.
4. Kaur M, Singh K. Review on titanium and titanium based alloys as biomaterials for orthopaedic applications. *Mater Sci Eng C*. 2019;102:844-862. doi:10.1016/j.msec.2019.04.064
5. Feller L, Jadwat Y, Khammissa RAG, Meyerov R, Schechter I, Lemmer J. Cellular responses evoked by different surface characteristics of intraosseous titanium implants. *Biomed Res Int*. 2015;2015:1-8.
6. Wang Q, Zhou P, Liu S, Attarilar S, Ma RL. Multi-scale surface treatments of titanium implants for rapid osseointegration: a review. *Nanomaterials*. 2020;10:1244.
7. Bosshardt DD, Chappuis V, Buser D. Osseointegration of titanium, titanium alloy and zirconia dental implants: current knowledge and open questions. *Periodontol 2000*. 2000;2017(73):22-40.
8. Le Guéhennec L, Soueidan A, Layrolle P, Amouriq Y. Surface treatments of titanium dental implants for rapid osseointegration. *Dent Mater*. 2007;23:844-854.
9. Meng H, Chien EY, Chien H. Dental implant bioactive surface modifications and their effects on osseointegration: a review. *Biomark Res*. 2016;4:1-14. doi:10.1186/s40364-016-0078-z
10. Nevins M. Clinical and histologic evaluations of immediately placed SLA dental implants. *Int J Periodontics Restorative Dent*. 2018;38:165-170.
11. Romero-Gavilán F, Sanchez-Pérez AM, Araújo-Gomes N, et al. Proteomic analysis of silica hybrid sol-gel coatings: a potential tool for predicting the biocompatibility of implants in vivo. *Biofouling*. 2017;33:676-689.
12. Chug A, Shukla S, Mahesh L, Jadwani S. Osseointegration-molecular events at the bone-implant interface: a review. *J Oral Maxillofac Surgery Med Pathol*. 2013;25:1-4. doi:10.1016/j.ajoms.2012.01.008
13. Gallagher WM, Lynch I, Allen LT, et al. Molecular basis of cell-biomaterial interaction: insights gained from transcriptomic and proteomic studies. *Biomaterials*. 2006;27:5871-5882.
14. Anitua E, Cerqueira A, Romero-gavilán F, et al. Influence of calcium ion-modified implant surfaces in protein adsorption and implant integration. *Int J Implant Dent*. 2021;7:1-11.
15. Zhen Z, Zheng Y, Ge Z, Lai C, Xi T. Biological effect and molecular mechanism study of biomaterials based on proteomic research. *J Mater Sci Technol*. 2017;33:607-615. doi:10.1016/j.jmst.2017.01.001
16. Othman Z, Mohren RJC, Cillero-Pastor B, et al. Comparative proteomic analysis of human mesenchymal stromal cell behavior on calcium phosphate ceramics with different osteoinductive potential. *Mater Today Biol*. 2020, 7;7:100066. doi:10.1016/j.mtbio.2020.100066
17. Kim CS, Lee KJ, Kim JE, Park YG, Ryu JJ, Kim HR. Proteomic analysis of the biological response of MG63 osteoblast-like cells to titanium implants. *Odontology*. 2014;102:241-248.
18. Zhao M, An M, Wang Q, et al. Quantitative proteomic analysis of human osteoblast-like MG-63 cells in response to bioinert implant material titanium and polyetheretherketone. *J Proteom*. 2012;75:3560-3573. doi:10.1016/j.jprot.2012.03.033
19. Omidi M, Ahmad Agha N, Müller A, et al. Investigation of the impact of magnesium: versus titanium implants on protein composition in

osteoblast by label free quantification. *Metallomics*. 2020;12:916-934.
20. Zhao M, Wang Q, Lai W, et al. In vitro bioactivity and biocompatibility evaluation of bulk nanostructured titanium in osteoblast-like cells by quantitative proteomic analysis. *J Mater Chem B*. 2013;1:1926-1938.
21. Romero-Gavilán F, Gomes NC, Ródenas J, et al. Proteome analysis of human serum proteins adsorbed onto different titanium surfaces used in dental implants. *Biofouling*. 2017;33:98-111.
22. Wisniewski JR, Zougman A, Nagaraj N, Mann M, Wi JR. Universal sample preparation method for proteome analysis. *Nat Methods*. 2009;6:377-362. http://www.ncbi.nlm.nih.gov/pubmed/19377485
23. Cerqueira A, Romero-Gavilán F, Araújo-Gomes N, et al. A possible use of melatonin in the dental field: protein adsorption and in vitro cell response on coated titanium. *Mater Sci Eng C*. 2020;116:111262. doi:10.1016/j.msec.2020.111262
24. Araújo-Gomes N, Romero-Gavilán F, García-Arnáez I, et al. Osseointegration mechanisms: a proteomic approach. *J Biol Inorg Chem*. 2018;23:459-470. doi:10.1007/s00775-018-1553-9
25. Romero-Gavilan F, Araújo-Gomes N, Sánchez-Pérez AM, et al. Bioactive potential of silica coatings and its effect on the adhesion of proteins to titanium implants. *Colloids Surf B Biointerfaces*. 2017;162:316-325. http://linkinghub.elsevier.com/retrieve/pii/S0927776517308378
26. Hidalgo-Bastida LA, Cartmell SH. Mesenchymal stem cells, osteoblasts and extracellular matrix proteins: enhancing cell adhesion and differentiation for bone tissue engineering. *Tissue Eng – Part B Rev*. 2010;16:405-412.
27. Vandrovcová M, Bačáková L. Adhesion, growth and differentiation of osteoblasts on surface-modified materials developed for bone implants. *Physiol Res*. 2011;60:403-417.
28. Ge M, Ke R, Cai T, Yang J, Mu X. Identification and proteomic analysis of osteoblast-derived exosomes. *Biochem Biophys Res Commun*. 2015;467:27-32. doi:10.1016/j.bbrc.2015.09.135
29. Baird TD, Wek RC. Eukaryotic initiation factor 2 phosphorylation and translational control in metabolism. *Adv Nutr*. 2012;3:307-321.
30. Weber JA, Gay CV. Expression of translation initiation factor IF2 is regulated during osteoblast differentiation. *J Cell Biochem*. 2001;81:700-714.
31. Sattlegger E, Hinnebusch AG. Separate domains in GCN1 for binding protein kinase GCN2 and ribosomes are required for GCN2 activation in amino acid-starved cells. *EMBO J*. 2000;19:6622-6633.
32. Hamamura K, Tanjung N, Yokota H. Suppression of osteoclastogenesis through phosphorylation of eukaryotic translation initiation factor 2 alpha. *J Bone Miner Metab*. 2013;31:618-628.
33. Bakker AD, Gakes T, Hogervorst JMA, de Wit GMJ, Klein-Nulend J, Jaspers RT. Mechanical stimulation and IGF-1 enhance mRNA translation rate in osteoblasts via activation of the AKT-mTOR pathway. *J Cell Physiol*. 2016;231:1283-1290.
34. Chen J, Long F. MTOR signaling in skeletal development and disease. *Bone Res*. 2018;6:1-6.
35. Pantovic A, Krstic A, Janjetovic K, et al. Coordinated time-dependent modulation of AMPK/Akt/mTOR signaling and autophagy controls osteogenic differentiation of human mesenchymal stem cells. *Bone*. 2013;52:524-531. doi:10.1016/j.bone.2012.10.024
36. Mu Z, Wang L, Deng W, Wang J, Wu G. Structural insight into the ragulator complex which anchors mTORC1 to the lysosomal membrane. *Cell Discov*. 2017;3:17049. doi:10.1038/celldisc.2017.49
37. Li J, Kim SG, Blenis J. Rapamycin: one drug, many effects. *Cell Metab*. 2014;19:373-379. doi:10.1016/j.cmet.2014.01.001
38. Chen J, Holguin N, Shi Y, Silva MJ, Long F. mTORC2 signaling promotes skeletal growth and bone formation in mice. *J Bone Miner Res*. 2015;30:369-378.
39. Piercy-Kotb SA, Mousa A, Al-Jallad HF, et al. Factor XIIIA transglutaminase expression and secretion by osteoblasts is regulated by extracellular matrix collagen and the MAP kinase signaling pathway. *J Cell Physiol*. 2012;227:2936-2946.
40. Isenberg JS, Roberts DD. THBS1 (thrombospondin-1). *Atlas Genet Cytogenet Oncol Haematol*. 2020;1:291-299.
41. Calabro NE, Kristofik NJ, Kyriakides TR. Thrombospondin-2 and extracellular matrix assembly. *Biochim Biophys Acta – Gen Subj*. 2014;1840:2396-2402.
42. Stenina-Adognravi O, Plow EF. Thrombospondin-4 in tissue remodeling. *Matrix Biol*. 2019;75-76:300-313. doi:10.1016/j.matbio.2017.11.006
43. Murphy-Ullrich JE. Thrombospondin 1 and its diverse roles as a regulator of extracellular matrix in fibrotic disease. *J Histochem Cytochem*. 2019;67:683-699.
44. Lin X, Patil S, Gao YG, Qian A. The bone extracellular matrix in bone formation and regeneration. *Front Pharmacol*. 2020;11:1-15.
45. Pereira AR, Lipphaus A, Ergin M, et al. Modeling of the human bone environment: mechanical stimuli guide mesenchymal stem cell–extracellular matrix interactions. *Materials*. 2021;14:4431.
46. Mizuno M, Kuboki Y. Osteoblast-related gene expression of bone marrow cells during the osteoblastic differentiation induced by type I collagen. *J Biochem*. 2001;129:133-138.
47. Ghanem A, Lu Y, Cai T, Mu X. Overexpression of RBP4 promotes proliferation, differentiation and mineralization of MC3T3-E1. *Int J Clin Exp Pathol*. 2017;10:298-305.
48. Chen L, Jiang W, Huang J, et al. Insulin-like growth factor 2 (IGF-2) potentiates BMP-9-induced osteogenic differentiation and bone formation. *J Bone Miner Res*. 2010;25:2447-2459.
49. Xiao H, Chen J, Duan L, Li S. Role of emerging vitamin K-dependent proteins: growth arrest-specific protein 6, Gla-rich protein and periostin (review). *Int J Mol Med*. 2021;47:1-17.
50. Mackie EJ, Ramsey S. Modulation of osteoblast behaviour by tenascin. *J Cell Sci*. 1996;109:1597-1604.
51. Kidwai F, Mui BWH, Arora D, et al. Lineage-specific differentiation of osteogenic progenitors from pluripotent stem cells reveals the FGF1-RUNX2 association in neural crest-derived osteoprogenitors. *Stem Cells*. 2020;38:1107-1123.
52. Kim JM, Yang YS, Park KH, Oh H, Greenblatt MB, Shim JH. The ERK MAPK pathway is essential for skeletal development and homeostasis. *Int J Mol Sci*. 2019;20:1803.
53. Yamashita T, Kamada H, Kanasaki S, et al. Ephrin type-a receptor 2 on tumor-derived exosomes enhances angiogenesis through the activation of MAPK signaling. *Pharmazie*. 2019;74:614-619.
54. Han J, Wang L, Lv H, et al. EphA2 inhibits SRA01/04 cells apoptosis by suppressing autophagy via activating PI3K/Akt/mTOR pathway. *Arch Biochem Biophys*. 2021;711:109024. doi:10.1016/j.abb.2021.109024

SUPPORTING INFORMATION

Additional supporting information can be found online in the Supporting Information section at the end of this article.

How to cite this article: Romero-Gavilán F, Cerqueira A, García-Arnáez I, et al. Proteomic evaluation of human osteoblast responses to titanium implants over time. *J Biomed Mater Res*. 2022;1-15. doi:10.1002/jbm.a.37444